doi:10.1016/S0301-5629(02)00704-4

● *Original Contribution*

IMPLEMENTATION ISSUES IN ULTRASONIC FLOW IMAGING

S. K

simpler hardware implementation (Alam and Parker 1996). A detailed analysis and comparison with the conventional methods are presented in Alam (1996).

Under a number of specific assumptions and key modifications, the WMLE could be modified into the form of the butterfly search on quadrature components (Alam and Parker 1995). Discrete radon transform, which has uses in beamforming (Johnson and Dudgeon 1993), could also be related logically to the butterfly search. See Durrani and Bisset (1984) for an overview of radon transform and its properties.

Tracking methods have been found to perform well. Some of these methods suffer from notable limitations, including aliasing effects in the 2-D Fourier fast transform and the necessity to accurately know the received signal shape in the WMLE. These methods are, typically, computation-intensive; however, with the recent advances in processing speeds, this may not be a significant limitation.

Butterfly search

A simplified 1-D model was used in Alam and Parker (1995) to derive the butterfly search estimator. For a point target moving toward the transducer, if the velocity v_0 is constant, then the nth RF A-line can be shown to have the following form:

$$s\ n,\ t) = A\cos\left[\omega_0\left[t - 2\,\frac{d}{c} + 2n\,\frac{\nu_0}{c}\,T\right]\right] \times r\left[t - 2\,\frac{d}{c} + 2n\,\frac{\nu_0}{c}\,T\right],\ n = 0,1,2,\cdots,N-1, \quad (1)$$

where A is the signal amplitude, n is the index for the repeated transducer bursts, T is the pulse-repetition period, d is the distance of the object from the transducer at the first transducer burst ($n = 0$), ω_0 is the angular center frequency, c is the sound propagation speed, and $r(\ )$ is the envelope of the transmitted pulse (frequently modeled as Gaussian, maximizing at $t = 0$). The factor of 2 in the expression comes from the round-trip travel of the wave. Time-axis origin is reset at each transducer burst. System effects are neglected.

For the RF signal in eqn (1), the complex envelope can be expressed as:

$$\tilde{r}\ n,\ t) = \tilde{A}\exp - j\left[2\omega_0 n\,\frac{\nu_0}{c}\,T\right]r\left[t - 2\,\frac{d}{c} + 2n\,\frac{\nu_0}{c}\,T\right], \quad (2)$$

where

$$\tilde{A} = \frac{A}{2}\exp j\left[2\omega_0\,\frac{d}{c}\right]. \quad (3)$$

This signal can be resampled at depth d along trajectories describing lines of constant velocity in (n, t) space. If $\tilde{r}_{Bv}[n]$ denotes the resampling of the complex envelope along the line for velocity v:

$$\tilde{r}_{Bv}[n] = \tilde{r}\ n,\ t)\big|_{t=2\frac{d}{c}-2n\frac{\nu}{c}T} = \tilde{A}\ \exp - j\left[2\omega_0 n\,\frac{\nu_0}{c}\,T\right]r\left[2n\,\frac{\nu_0 - \nu}{c}\,T\right]. \quad (4)$$

When $\nu = \nu_0$, $\tilde{r}_{B\nu_0}[$ t

RF A-line. Because of the relatively long wavelength of 5-MHz pulses, the point scatterer model is a good approximation; it would be less accurate at higher (*e.g.*, $>$ 50 MHz) transducer frequencies (Hunt et al. 1995). Figure 1 shows the cross-sectional view of the 3-D scattering volume of simulation geometry. A cylindrical vessel, carrying the moving scatterers, is embedded in the tissue comprised strong stationary scatterers (clutter). The vessel axis lies on the image plane and is at an angle θ_0 with the direction of propagation; thus, lateral movement of the scatterers will produce some speckle decorrelation. The effects of US beam geometry (*e.g.*, focusing, sidelobes, grating lobes) and the frequency-dependent attenuation of the intervening tissue were ignored. The beam is Gaussian in both lateral and azimuthal directions. In short, the simulation consists of 3-D random scatterers convolved with a nondiffracting 3-D acoustic pulse (1-mm beam width). The velocity profile is parabolic ($\nu = V_{\max}[1 - (r/R)^2]$). In the simulation we used, r = 0.5 cm, $\theta_0 = 45°$ and $V_{\max} = 100$ cm/s. For the simulated 2-way pulse, $f_0 = 4$ MHZ, bandwidth = 56% (-6 dB). Number of A-lines = 3, and SNR = 3 dB. (Maximum velocity in the direction of propagation was 70.71 cm/s.) The ratio of stationary clutter to moving scatterer strength was 40 dB (*i.e.*, the moving "blood" is hypoechoic). RF echo signals were sampled at 40×10^6 cycles/s. No vessel wall was simulated. The velocity of each scatterer was assumed unchanged through the scanning process. A scatterer concentration of 64 mm^{-3} was used. The initial 1-D simulation model used a similar two-way acoustic pulse (5-MHz center frequency and 56% fractional bandwidth), unless indicated otherwise; a total of 67 scatterers/mm were simulated, which was more than sufficient for fully developed speckle. $f_s = 50 \times 10^6$

In Fig. 3, results from 1-D simulation are shown to demonstrate the effect of bandwidth and chirps instead of regular pulses. Only Fig. 3f has additive noise (SNR = 0 dB). At a lower σ (pulse envelope: $r(t) = e^{-2(\pi\sigma t)^2}$), the subsidiary peaks of $L(\nu)$ are comparable to the primary peak. On the other hand, use of chirps produces lower subsidiary peaks at low σ. However, at higher σ, perhaps because the bandwidth is high to begin with, improvements are minimal. When the number of A-lines is increased, the primary peak becomes sharper; however, it does not noticeably affect the height of the subsidiary peaks. With the addition of noise, the base level of $L(\nu)$ increases. Thus, the butterfly search can be directly applied to the reflected echoes for chirp transmission. And, because the butterfly search is a broadband method, it can also be applied after pulse compression processing.

Wall filtering

Suppression of "clutter" is a major issue in color flow imaging. Clutter refers to the strong echo signal from the stationary or slowly moving wall and tissues close to vessel walls. Even when the sample volume is farther away from the vessel walls than the width of the system impulse response, clutter might still be present due to the 3-D nature of sample volume, sidelobes, refraction, multiple reflections, range ambiguity, etc. Unless adequately suppresshe issuetosevo(suca8[(ections,)-236.Tu2Sai

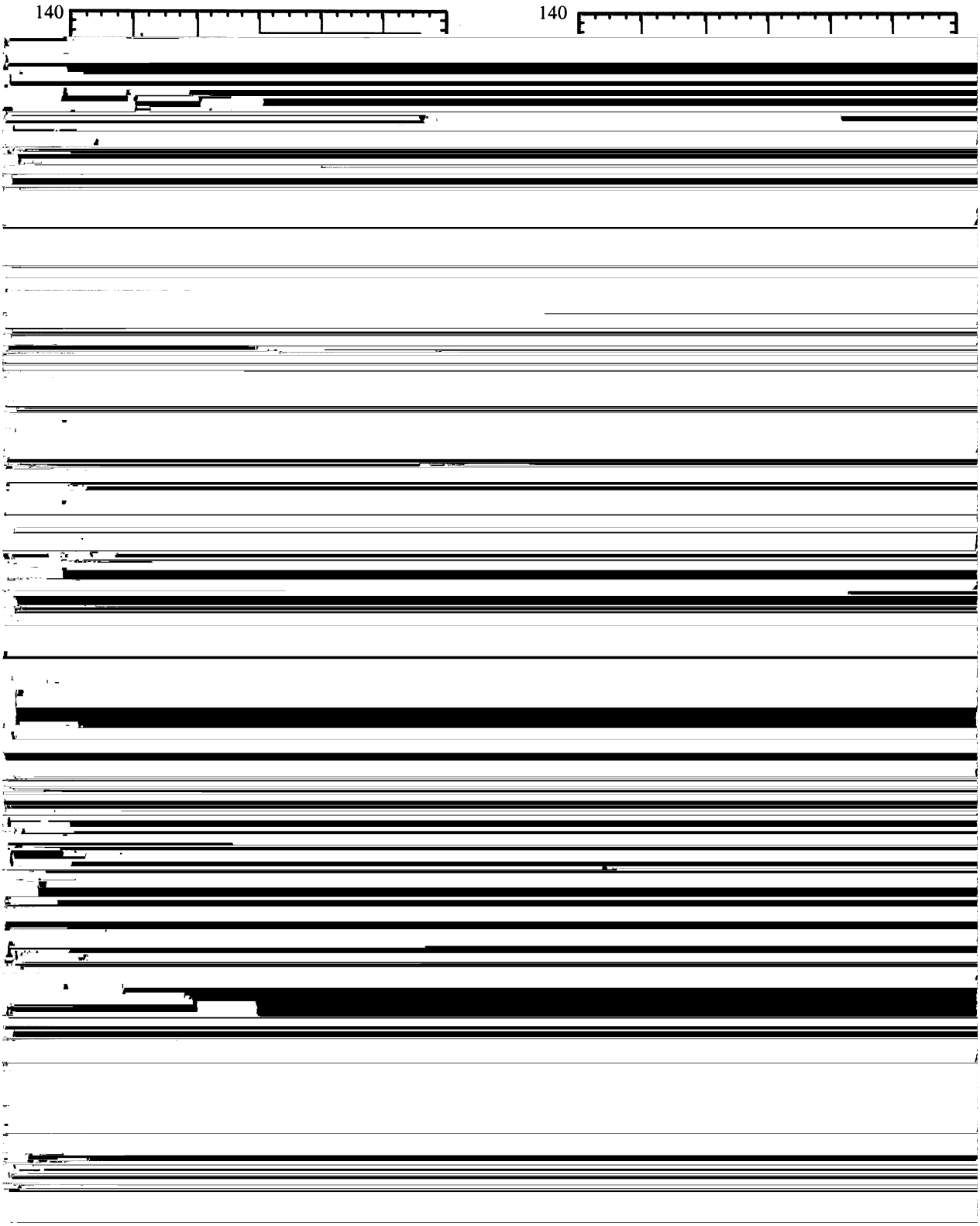

Fig. 3. (a) $L(\nu)$ for a narrowband pulse (σ = 0.41 MHz). Number of lines = 4. (b) Chirp (σ = 0.41 MHz, f = 1.34 MHz/μs). Number of lines = 4. (c) Wideband pulse (σ = 1.41 MHz). Lines = 4. (d) Chirp (σ = 1.41 MHz, f = 3.33 MHz/μs). Lines = 4. (e) Wideband pulse (σ = 1.41 MHz). Lines = 8. (f) Wideband pulse (σ = 1.41 MHz). Lines = 4, SNR = 0 dB.

y search technique can detect the ow of hypoechoic blood without wall ltering in the proximity of vessel walls. First, we will show the effect of clutter on L( ). Then, we will show that butter y search can detect ow close to vessel walls in large vessels. We will also show, using color ow images, that the butter y search can detect blood ow in small vessels without wall ltering.

Figure 4a–g plots L(

well it approximates the clutter component. A few articles discussed step-initialized IIR lters (Shariati et al. 1993), evaluation of IIR initialization schemes (Peterson et al. 1994), and adapting wall ltering to the mean frequency of the tissue component (Thomas and Hall 1994). Kadi and Loupas (1995) compared the performances of regression lters and IIR lters; wall lter performance generally depends heavily on the clutter-to-signal ratio and improves significantly when the number of A-lines is increased.

We have investigated wall ltering in the context of the butter y search. We have discovered that the butter-

close to the wall is slow, primary peak of $L(\nu)$, which depends on the combined effect of slow-moving blood and stationary tissue, will show presence of flow. However, as shown in Table 1, interaction of the contribution from tissue and blood will bias these flow estimates (toward smaller values), which should be investigated further in the future.

Figure 5 shows the duplex (color Doppler superimposed on B-mode) images for the same 3-D model for the butterfly search and autocorrelation technique. We have used standard red and blue color codes for all flow images. The autocorrelation technique suffers from aliasing and large estimation errors. The butterfly search duplex image clearly depicts the parabolic flow profile. These images also show that the butterfly search detects flow close to the wall, whereas the autocorrelation method does not.

Figure 6 further exhibits the ability of the butterfly search technique in detecting blood flow in small vessels without wall filtering. A 1-mm vessel was simulated carrying plug flow (7.07 cm/s in the beam direction). Other parameters were the same as the prior simulation. The autocorrelation technique failed to show blood flow in the vessel. On the other hand, the red color within the vessel depicts the blood flow in the vessel when the butterfly search was used. Clearly, contribution from clutter has introduced bias in the peak of $L(\nu)$; estimated velocities were $\approx$1 cm/s inside the vessel. However, detection of flow is frequently enough for diagnosis and, in such cases, the bias is not a significant issue. The decreased need for a wall filter is a practical and computational advantage.

ESTIMATOR PERFORMANCE

One-dimensional plots of results inES9.2(reat cu9D -339.2-2.pa.wall,)-6il practical

plotted for SNR = 20 dB and SNR = 3 dB in Fig. 8 (number of lines = 3). As expected, we observe that the original butterfly search has the lowest SD, followed closely by the simplified butterfly search at both SNR levels. Notice the different vertical scales for different graphs, especially for RF correlation search at 3 dB. Both the autocorrelation and RF correlation search perform poorly at 3 dB. The autocorrelation method shows large variations even at 20 dB. The cross-correlation technique has large variance close to the wall at 3 dB. We postulate this to be due to higher velocity gradients in the region. M-mode images are created for all the four techniques from these estimated profiles (Fig. 9). The butterfly search methods show the lowest variation in estimated profile with time (horizontal axis).

DISCUSSION AND CONCLUSION

Various practical issues regarding the implementation of flow imaging are considered in this article. They include frequency-dependent scattering and attenuation, interpolation of $L(\nu)$ peak to reduce computation, use of chirps instead of regular pulses, and wall filtering issues.

The butterfly search technique has been shown to have excellent immunity to noise or other difficult conditions, including decorrelations using simulations and experiments even at a small number of A-lines. McAleavey and Parker (2001) investigated in detail the effect of decorrelation on the performance of the butterfly search. The method's high computational complexity is a limitation. Alam and Parker (1996) discussed two approaches to reduce computational complexity. Additionally, peak interpolation discussed in this article should provide additional reduction. The ability to accurately estimate flow using few A-lines can improve the frame rate of color flow imaging. However, for a given number of A-lines, frame rate is ultimately limited by the PRF due to the range ambiguity problems. In the presence of turbulent flows, since the group of scatterers in the sample volume can break up quickly, estimation is more accurate if it can be performed with few A-lines. At low SNR levels, false peaks in the

Embree PM, Mayo WT. Ultrasonic M-mode RF display technique with application to flow visualization. SPIE Int Symp Pattern Recog Acoust Imaging 1987;768:70–78.

Ferrara KW, Algazi VR. A new wideband spread target maximum likelihood estimator for blood velocity estimation—part I: Theory. IEEE Trans Ultrason Ferroelec Freq Control 1991a;38:1–16.

Ferrara KW, Algazi VR. A new wideband spread target maximum likelihood estimator for blood velocity estimation—Part II: Evaluation of estimators with experimental data. IEEE Trans Ultrason Ferroelec Freq Control 1991b;38:17–26.

Ferrara KW, DeAngelis G. Color flow mapping. Ultrasound Med Biol 1997;23:321–345.

Ferrara KW, Algazi VR, Liu J. The effect of frequency dependent scattering and attenuation on the estimation of blood velocity using ultrasound. IEEE Trans Ultrason Ferroelect Freq Control 1992;39: 754–767.

Foster SG, Embree PM, O'Brien WD Jr. Flow velocity profile via time-domain correlation: Error analysis and computer simulation. IEEE Trans Ultrason Ferroelec Freq Control 1990;37:164–175.

Hein IA, O'Brien WD Jr. Current time-domain methods for assessing tissue motion by analysis from reflected ultrasound echoes—a review. IEEE Trans Ultrason Ferroelec Freq Control 1993b;40:84–102.

Hunt JW, Worthington AE, Kerr AT. The subtleties of ultrasound images of an ensemble of cells: Simulation from regular and more –767.

Foster 1976–767138 T*JA.oel38 T*Det(ulf)-25938 T*1 Tbabiliof